Sensors and Materials, Vol. 36, No. 4 (2024) 1545–1555
MYU Tokyo

S & M 3617

Optimal Ground Control Point Utilization for Aligning 3D Surface Models of Forest Areas with Steep Slopes

Jeongjae Kim,[1] Ikhyun Kim,[1] and Byoungkoo Choi[2*]

[1]Department of Forestry and Environmental Systems, Kangwon National University, Chuncheon 24341, Republic of Korea
[2]Division of Forest Sciences, Kangwon National University, Chuncheon 24341, Republic of Korea

(Received Octobar 16, 2023; accepted March 28, 2024)

Keywords: unmanned aerial vehicle (UAV) photogrammetry, ground control point (GCP), timber harvesting, georeferencing, 3D surface model alignment

Unmanned aerial vehicles (UAVs) have been used to survey forests for decades. To monitor post-forest operation effects such as the surface deformation of forest soils (e.g., soil erosion and deposition), the alignment of 3D surface models using ground control points (GCPs) by georeferencing is necessary. However, the GCP network optimization for surveying forests has not been clearly established. We installed 29 GCPs on tree stumps in a post-timber harvesting site to spatially correct UAV survey results, for which real-time kinematics data were unavailable. The GCPs for georeferencing were randomly selected from 13 validation sets for each of the three trials in this study; the GCP and checkpoint root mean square errors (*RMSE*s) were used for determining the georeferencing results. Even if the number of GCPs increased, the GCP *RMSE* did not decrease; the checkpoint *RMSE* decreased by 2.03 cm. The 3D surface model alignment using 6 and 26 GCPs did not show a significant difference in alignment error (3.78 and 2.96 cm, respectively). Our results reveal that GCP *RMSE* does not affect the alignment error; therefore, we suggest using at least 6 GCPs for the precise alignment of 3D surface models while utilizing the same GCPs for aligning pre- and post-3D surface models.

1. Introduction

Forest operations can cause various disturbances to the forest environment. Heavy machines, which are essential for tree logging, can cause adverse environmental effects due to the rutting of forest soil.[1–4] Sustainable forest management requires continuous monitoring, especially after implementing forestry operations. For continuous monitoring, it is essential to conduct direct surveys (for detailed investigations and measurements). However, surveying forests with human effort is difficult because of the challenging terrain and limited available facilities in such areas.

To reduce the labor intensity in surveying forests, a 2D-sensor-based unmanned aerial vehicle (UAV) system was implemented in various forestry fields owing to their cost efficiency

*Corresponding author: e-mail: bkchoi@kangwon.ac.kr
https://doi.org/10.18494/SAM4705

ISSN 0914-4935
https://myukk.org/

when compared with 3D scanning sensors, such as LiDAR. Several attempts have also been made to introduce novel technologies for monitoring post-timber harvesting effects such as the elevation changes caused by the surface deformation of forest soils (e.g., soil erosion and deposition).[5,6] To detect the changes in soil surfaces, a few recent studies used UAV-derived 3D surface models to identify the wheel tracks of forestry machines (left behind after timber harvesting).[7,8] In this study, we collected approximately 200 2D images for monthly UAV surveys of the slope using UAV photogrammetry technology; a 3D surface model of the post-timber harvesting site was created using the structure from motion (SfM) photogrammetry algorithm, and the soil changes in the target site were also observed.[8] Moreover, ground control points (GCPs) were used to align the monthly point cloud data (PCD) acquired through georeferencing and calculate the elevation changes (e.g., erosion and deposition) in the soil surface.

The optimization of GCP installation and utilization has been studied in various industries to ensure accurate surveying and precise ground truth data.[9–11] A recent study carried out multiple simulations based on UAV photogrammetry to determine the optimization of GCP utilization; the study configured 24 GCP networks to confirm the optimal method of GCP use.[11] Although extensive studies have been conducted in various related fields, there is a lack of studies on the optimal installation and utilization of GCP methods in mountainous and forested terrains.

To monitor the topographical changes at the target site, enabling the continuous acquisition of 3D data is important; notably, in such cases, the technology used for data acquisition and the alignment of the acquired 3D data are the key factors. Therefore, in this study, we monitored the impact of post-timber harvesting operations on the forest environment using UAVs to determine the optimal number of GCPs required to effectively monitor an area. First, we used GCPs to implement a nonrestorative extraction method and obtained the spatial root mean square error (*RMSE*) for each number of GCPs utilized to confirm the optimal number. Then, after carrying out geometric correction by applying the same GCP used for the verification of the time-lapse data, the overlapping state of both PCD points was examined as the distance of the GCP identified in the orthomosaics to confirm the overlap accuracy according to the spatial *RMSE*.

2. Data, Materials, and Methods

2.1 Site description

We selected the forest area of Kangwon National University, Gangwon Province, Republic of Korea (37°46′34.4″ N, 127°49′41.1″ E) as our study area (Fig. 1). Approximately 3 ha of timber was harvested at the site in March 2022. The site has an altitude of 508–628 m above sea level, with an average slope of 47%. After clearcutting, stumps and logging debris remained on the slopes of the area, with the debris being arranged horizontally downslope. A real-time kinematic (RTK) system was not available for this region because of the mountainous site location, as the signal from the base station could not be received at the site. However, the GPS signals from the site could be recorded using satellites; therefore, we surveyed the area using a UAV.

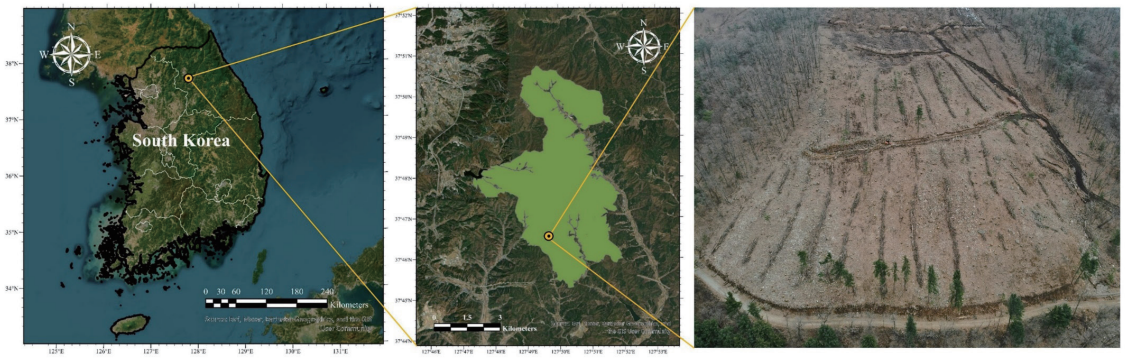

Fig. 1. (Color online) Location and panoramic view of the timber-harvesting area of Kangwon National University considered in Kim *et al.*[8] and this study.

2.2 UAV survey and field data collection

In this study, surveys were conducted using UAVs equipped with a global navigation satellite system (GNSS). The UAV survey was performed with DJI Matrice 300 (Da-Jiang Innovation, Shenzhen, China) as the platform and DJI Zenmuse H20T (Da-Jiang Innovation, Shenzhen, China) as the sensor. The DJI Matrice 300 weighed approximately 7 kg and provided with both GPS and RTK modes. The maximum flight duration of the DJI Matrice 300 attached with the DJI Zenmuse H20T was about 43 min. The DJI Zenmuse H20T weighed 0.82 kg and provided an optical camera with a resolution of 12 megapixels.

To georeference the 3D surface models derived from UAV surveys, a 40 × 40 cm^2 Fomex texture plate of 29 GCP markers was prepared for the preprocessing of the study site, where the RTK mode is unavailable. We selected stumps, which are undeforming objects for monitoring the forest field, to install GCP markers. During the GCP installation, we considered 1 GCP per 30 × 30 m^2 to cover approximately 3 ha of the total study site.

Vertically parallel flights were performed at heights of 100 and 140 m [Fig. 2(a)] for every monthly UAV survey with the GPS mode because of the unavailability of the RTK mode. The flight speed was set at 5 m/s, optimized for the battery duration of the DJI Matrice 300 RTK system. The overlaps were set to 90 and 80% on the front and back sides, respectively. The margins were set at 20 m to ensure the high quality of the PCD during processing. The coordinates of the GCP points were collected to validate the georeferencing results. On the other hand, field survey was conducted with Trimble R12i GNSSs (Trimble, Westmister, USA). The spatial coordinates of GCPs (with the least coordinate error of 3 cm) were collected using GNSS from the center point of each GCP marker [Fig. 2(b)].

2.3 Photogrammetric process

The photogrammetric process was performed using Agisoft Metashape ver.1.7.4 (Agisoft LLC., Petersburg, Russia) (Table 1). Using the SfM algorithm, we first simulated sparse clouds

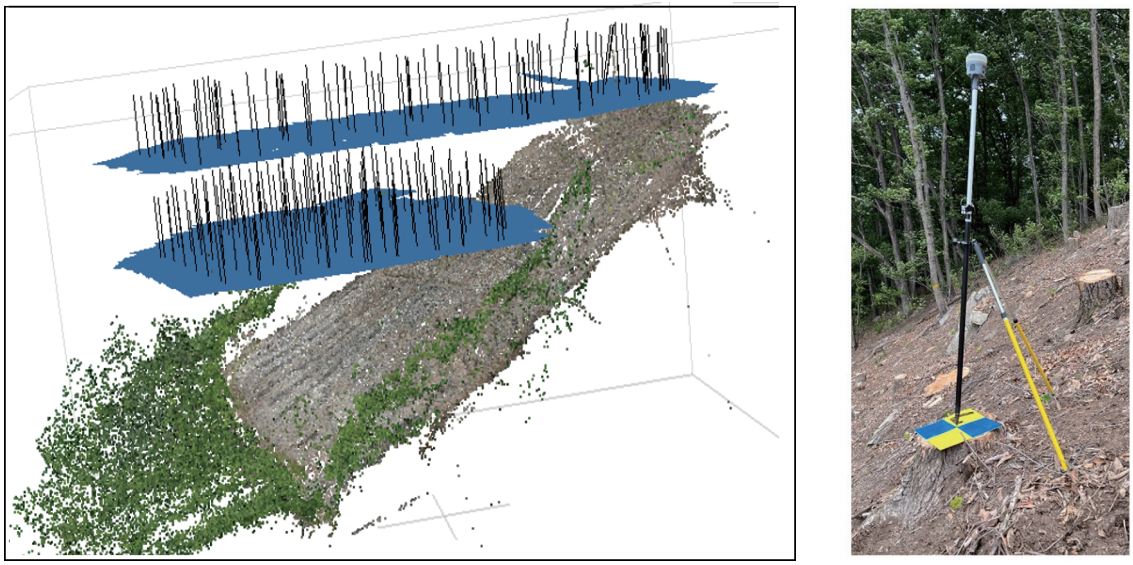

(a) (b)

Fig. 2. (Color online) Illustration of the surveying method carried out in this study using UAVs and field references, which was the same as the method used by Kim *et al*.:[8] (a) shows a vertically parallel flight for monthly UAV surveys and (b) shows the GCP–GNSS survey carried out using GCPs installed on tree stumps in the study area.

Table 1
Parameters used in each process to generate 3D data.

Process	Parameter	Setting
Align Photos	2D image input	140 m + 100 m
	Accuracy	Highest
	Reference preselection	On
	Key-point limit	40000
	Tie-point limit	4000
Build Dense Cloud	Quality	Ultrahigh
	Depth filtering	Aggressive
Build DSM	Projection	WSG 84 (EPSG: 4326)
	Source data	Dense cloud
	Point classes	All
Build Orthomosaic	Projection	WSG 84 (EPSG: 4326)
	Surface	DEM

*Abbreviations: digital surface model (DSM); World Geodetic System 1984 (WSG 84), European Petroleum Survey Group (EPSG), digital elevation model (DEM)

from 235 2D images captured in July 2022 and 230 2D images captured in September 2022. By calculating the coordinates and correlations of the 2D images, generally referred to as PCD points, we simulated dense clouds from the data of sparse clouds. The PCD points were subsequently generated into digital surface models (DSMs) and orthomosaics by calculating the height of each PCD point and the color of each pixel point from the 2D images.

2.4 Georeferencing by sampling without replacing GCPs

The number of GCPs required for optimum 3D surface model alignment was validated using two different methods: (1) random GCP selection for georeferencing and (2) the calculation of alignment error. The optimization results of the GCP configuration were compared on the basis of the number of GCPs utilized for data collection. In related studies, the number of validated GCPs was not unified.[11,12] However, the checkpoints and validated GCPs were assessed on the basis of spatial errors, which were calculated using the *RMSE*s of the *XYZ* coordinates.[11] Thus, for analyzing the probabilistic equity, we randomly sampled 4–28 GCPs in two multiples and calculated the GCP and checkpoint *RMSE*s in three different trials. To calculate the spatial *RMSE*s, the total coordinates of the 3D surface model GCPs were compared with those of the GNSS-GCPs (i.e., ground truth data) using the *XYZ* coordinate data. The equation for calculating the *RMSE*s of the 3D surface model GCPs from the ground truth is

$$RMSE_{xyz} = \sqrt{\frac{1}{n}\sum_{i=1}^{n}\Sigma\left(\Delta X_i^2 + \Delta Y_i^2 + \Delta Z_i^2\right)}, \tag{1}$$

where

ΔX_i = residual of ith value for X-axis,
ΔY_i = residual of ith value for Y-axis,
ΔZ_i = residual of ith value for Z-axis,
n = number of control points.

The purpose of georeferencing was to align the 3D surface model as precisely as possible to detect the surface deformations caused by the events that occurred in the region. Notably, the georeferencing process in multiple 3D surface models can automatically align multiple DSMs from different periods. However, determining the GCP center points in PCD is impossible with the automatic method. Therefore, the precision of the alignment was assessed by manually calculating the spatial distance between the GCP center points of the aligned orthomosaics in ArcGIS Pro.

3. Results and Discussion

The GCPs used for georeferencing were selected in two multiples (from 4 to 28); thus, the GCP networks were classified into 13 validation sets. The GCPs used for georeferencing each validation set were randomly selected by confirming the center of the GCP markers in the PCD acquired in July 2022 (Fig. 3). Because of vegetation growth, a few GCPs (e.g., GCP-1 and GCP-4) could not be identified clearly in the September 2022 orthomosaic. Thus, in the georeferencing of the September data, we excluded GCP-1 and GCP-4 for georeferencing the 3D surface models.

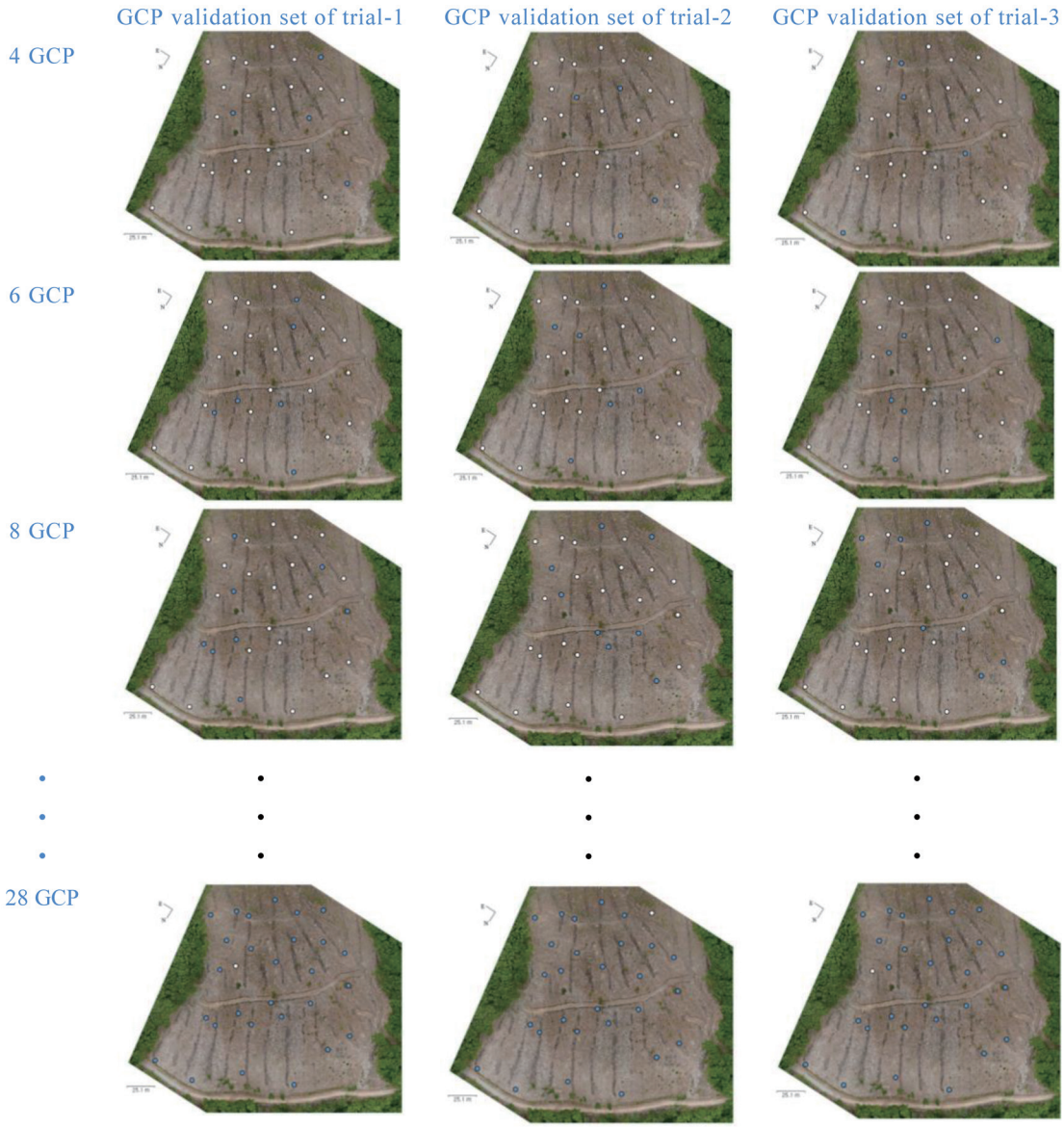

Fig. 3. (Color online) GCP network designs from random GCP selection. The GCPs (4–28) were selected on each GCP network by multiples of 2 in three different trials.

The georeferencing *RMSE* of each validation set was used to calculate the average *RMSE* (Fig. 4). Despite the increasing number of GCPs, the GCP *RMSE*s among all the GCP network designs did not vary significantly. In contrast, the checkpoint *RMSE* decreased by 2.03 cm until 26 GCPs were used. Moreover, the two validation sets confirmed precise georeferenced GCP networks by subtracting the GCP *RMSE* from the checkpoint *RMSE*. The lowest GCP and checkpoint *RMSE*s of all the GCP network designs were 6 GCP (10.69 and 14.52 cm, respectively), 14 GCP (11.21 and 15.24 cm, respectively), 16 GCP (11.62 and 14.83 cm, respectively), 20 GCP (12.09 and 16.53 cm, respectively), and 26 GCP (12.62 and 14.83 cm, respectively).

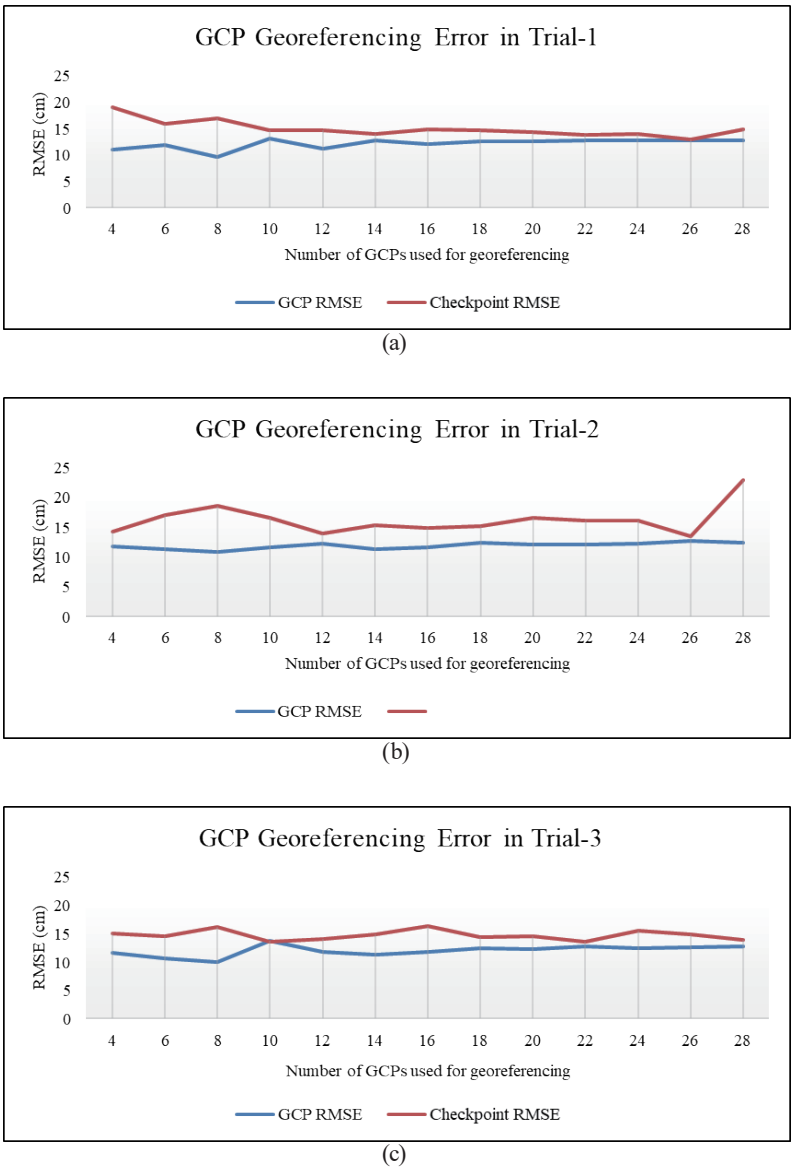

Fig. 4. (Color online) GCP and checkpoint *RMSE*s in the three validation sets considered in this study.

Despite the increase in the number of GCPs, we noted no reduction in GCP *RMSE* compared with the results of related GCP studies.[11–13] Although the results were shown as RMS in Hastaoglu *et al.*,[12] a comparison of checkpoint RMS data obtained for all-network design (46 GCPs) and sparse network design (32 GCPs) showed differences by an average of 2.87 cm when additional 14 GCPs were used from the sparse network design. In the comparison between the 4-GCP group and the 10-GCP or more group, which was presented by Zhang *et al.*,[13] the total horizontal error was reduced by an average of 30.63 cm. In particular, Villanueva and Blanco[11] investigated the optimization of GCP networks with various patterns (e.g., clumped – center, distributed – edge, clumped – edge, and distributed – edge and center), which was different from our study. The GCP *RMSE* of the study decreased significantly (by 1.6 m) with increasing

number of GCPs. Moreover, Villanueva and Blanco[11] revealed that the GCP *RMSE* results showed a significant reduction (by approximately 20 cm) from GCP 4 to GCP 24 of the *XY* coordinates, which is comparably similar to our study. However, the GCP *RMSE*s of *XY* and *Z* may not be perfectly comparable to those in our study because we considered the total *RMSE* of the *XYZ* coordinates. Thus, we compared the total GCP *RMSE* magnitude and noted a reduction of approximately 4 m. This result indicated that the DEM resolution of the comparison study was 10 cm, which was higher than that considered in our study (which is approximately 2.7 cm), and that the center points in our study may have been confirmed more precisely than the comparison site. Furthermore, the DSM resolution acquired for our study was significantly lower than that in the compared study by approximately 6.3 cm, which may have also affected the insignificant differences in GCP *RMSE*s in the 13 validation sets (Fig. 4). However, the checkpoint *RMSE* in our study showed a decreasing trend, similar to that in the compared studies.

Furthermore, we generated orthomosaics from all GCP validation sets for June and September 2022 by comparing the lowest GCP-*RMSE* of each GCP used for georeferencing (Table 2). The precision of the alignment was assessed using the orthomosaics for June and September 2022 (Table 2). The average alignment distances of the validation sets using 6 GCPs (VS-6) and 26 GCPs (VS-26) were calculated as 3.78 and 2.96 cm, respectively; the GCP-26 set was confirmed to be the most precisely aligned PCD (based on the total validation process).

Georeferencing is a key process that allows the alignment of different 3D surface models for effective monitoring;[14] the total alignment error in the study was 1.28–3.33 cm in the construction field. The lowest alignment errors in the *XY* and Z coordinates in an artificial mound, considered an idealized field condition, were calculated to be in the ranges of 1.31–3.39 cm for the *XY* error and 0.94–1.8 for the *Z* error (when using GCPs on the alignment).[15] A recent study that monitored timber-harvesting sites utilized 29 GCPs for georeferencing to align four different PCD points;[8] the results indicated that the alignment error for models developed for June and September 2022 was 3 cm. This error may be compared with that calculated as 2.96

Table 2
RMSE and alignment error estimated from the confirmed validation set of the lowest average GCP-checkpoint *RMSE*.

	Validation set-3 using 6 GCPs	Validation set-2 using 14 GCPs	Validation set-2 using 16 GCPs	Validation set-2 using 20 GCPs	Validation set-3 using 26 GCPs
GCPs used for survey	9, 11, 14, 20, 21, 27	3, 4, 5, 6, 7, 9, 12, 13, 14, 18, 20, 22, 24, 25	3, 5, 7, 9, 10, 12, 13, 14, 15, 17, 19, 21, 23, 24, 28, 29	1, 4, 7, 8, 10, 11, 12, 14, 16, 17, 18, 19, 21, 22, 23, 24, 25, 26, 28, 29	1, 2, 3, 4, 5, 6, 7, 8, 9, 10, 11, 12, 14, 15, 16, 18, 19, 20, 21, 22, 23, 24, 25, 27, 28, 29
Average GCP-checkpoint *RMSE* for June and September (cm)	4.5	2.94	3.52	2.82	1.02
Standard deviation of GCP-checkpoint for June and September (cm)	1.01	1.509	0.91	1.44	1.07
Average alignment error (cm)	3.78	3.85	3.74	3.63	2.96

cm for VS-26 in our study [Fig. 5(a)]. Our alignment error calculated for 3rd VS-26 was the most accurate validation set, with the error being less than 4 cm, according to related studies.[8,15] Moreover, the alignment error of the VS-6 was also acceptable compared with that of the VS-26 (Fig. 5). This result indicates that reducing the number of GCPs used for georeferencing may not negatively affect the alignment results when the post-3D surface model is generated from the same GCPs that were utilized in the pre-3D surface model, which was the approach adopted in this study.

Furthermore, we determined the optimal number of GCPs required for aligning the 3D surface models. A comparison of the average GCP-checkpoint *RMSE*s of the VS-6 and VS-26 showed a strong relationship with respect to the alignment error; the GCP-checkpoint *RMSE* of the VS-26 was approximately 3.48 cm lower than that of the VS-6 (Table 2). The decreasing gap between the GCP and checkpoint *RMSE*s also decreased the alignment error by 0.82 cm with respect to the average GCP-checkpoint *RMSE*. However, the standard deviation of the VS-6 and VS-26 validation sets was approximately 1 cm, indicating an insignificant difference. Furthermore, we confirmed that the VS-14, VS-16, and VS-20 sets had sufficiently small (<4 cm) alignment errors in the validation results (Table 2). Moreover, no significant difference was confirmed in the alignment performance (e.g., average GCP-checkpoint *RMSE*, standard deviation, and alignment error) of five cases (e.g., VS-6, VS-14, VS-16, VS-20, and VS-26) (Table 2). These results indicated no significant correlation between georeferencing and the

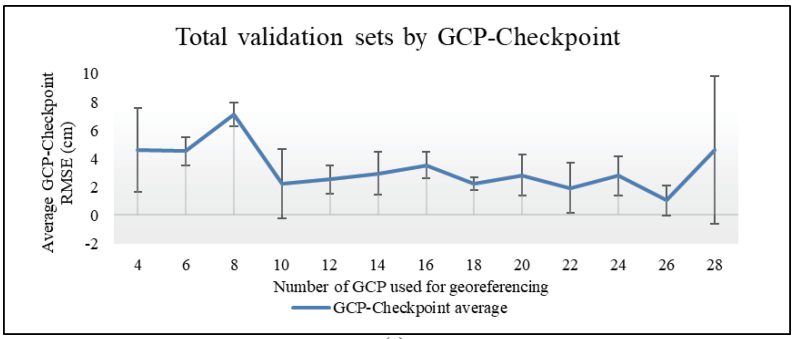

(a)

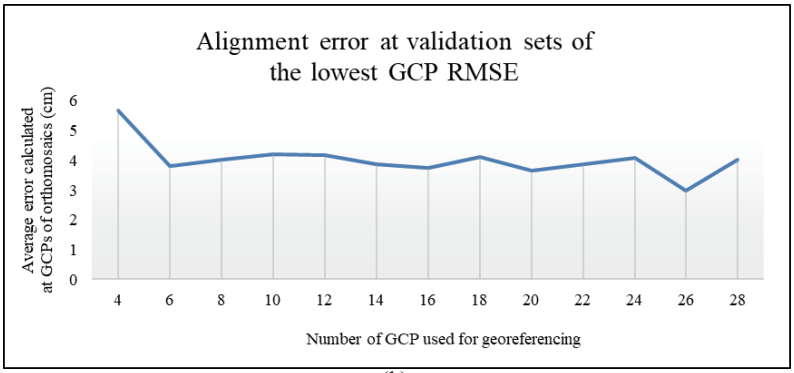

(b)

Fig. 5. (Color online) Comparison of GCPs and checkpoints in average *RMSE* and alignment error: (a) total *RMSE* of GCPs and checkpoints; error bars represent standard deviation and (b) average GCP-checkpoint *RMSE*.

number of GCPs. Another GCP-based 3D data alignment study indicated that using 6 GCPs for the alignment of multi-photogrammetry data at construction sites was possible; this approach is considered to be effective even in larger areas.[16] Thus, we conclude that the georeferencing method used in this study, wherein we considered the same GCPs used for collecting the PCD in June 2022 to collect the PCD in September 2022, could yield low alignment errors. We also conclude that the least alignment error can be acquired using 26 GCPs; however, similar results can be obtained using 6 GCPs.

4. Conclusions

The installation of GCPs in actual forest fields is not easy, as finding undeformed but sturdy objects is difficult. This can affect the distribution of GCPs in the field and the precision of the georeferencing results for the target site. To address this problem, we generated a total of 13 validation sets in three trials through random selection and assessed the GCP *RMSE* for each of the 13 validation sets; the results did not show significant differences. The alignment error confirmed from the generated visual 3D surface models, which were orthomosaics, showed no correlation with the GCP *RMSE* when the same GCPs were used for surveys during two different periods. Notably, we conclude that the GCP georeferencing methods and analysis results of this study can be utilized as base data for conducting or comparing UAV surveys in forest fields for which RTK data were not available. We suggest the use of more than 6 GCPs for georeferencing and aligning 3D surface models. Furthermore, we suggest using the same GCPs for developing the pre- and post-3D surface models. Although the proposed method can yield precise alignment results, validating this method by applying it to other forest areas in future studies is important.

Acknowledgments

This study was supported by the R&D Program for Forest Science Technology (Project Nos. 2021367B10-2323-BD01 and 2019151D10-2323-0301) of the Korea Forest Service (Korea Forestry Promotion Institute).

References

1 C. Nugent, C. Kanali, P. Owende, M. Nieuwenhuis, and S. Ward: For. Ecol. Manage. **180** (2003) 85. https://doi.org/10.1016/S0378-1127(02)00628-X
2 M. Cambi, G. Certini, F. Neri, and E. Marchi: For. Ecol. Manage. **338** (2015) 124. https://doi.org/10.1016/j.foreco.2014.11.022
3 B. Klaes, J. Struck, R. Schneider, and G. Schüler: Eur. J. For. Res. **135** (2016) 1083. https://doi.org/10.1007/s10342-016-0995-2
4 E. Marra, M. Cambi, R. Fernandez-Lacruz, F. Giannetti, E. Marchi, and T. Nordfjell: Scand. J. For. Res. **33** (2018) 613. https://doi.org/10.1080/02827581.2018.1427789
5 A. Salmivaara, M. Miettinen, L. Finér, S. Launiainen, H. Korpunen, S. Tuominen, J. Heikkonen, P. Nevalainen, M. Sirén, J. Ala-Ilomäki, and J. Uusitalo: Int. J. of For. Eng. **29** (2018) 41. https://doi.org/10.1080/14942119.2018.1419677
6 M. Pierzchała, B. Talbot, and R. Astrup: Forestry **89** (2016) 383. https://doi.org/10.1093/forestry/cpw009
7 S. Bhatnagar, S. Puliti, B. Talbot, J. B. Heppelmann, J. Breidenbach, and R. Astrup: Forestry **95** (2022) 698. https://doi.org/10.1093/forestry/cpac023

8 J. Kim, I. Kim, B. Choi: Forests. **14** (2023) 980. https://doi.org/10.3390/f14050980
9 G. Rossi, L. Tanteri, V. Tofani, P. Vannocci, S. Moretti, and N. Casagli: Landslides **15** (2018) 1045. https://doi.org/10.1007/s10346-018-0978-0
10 D. Turner, A. Lucieer, and S. M. De Jong: Rem. Sens. **7** (2015) 1736. https://doi.org/10.3390/rs70201736
11 J. K. S. Villanueva and A. C. Blanco: The International Archives of the Photogrammetry, Remote Sensing and Spatial Information Sciences **42** (2019) 167. https://doi.org/10.5194/isprs-archives-XLII-4-W12-167-2019
12 K. O. Hastaoglu, H. S. Kapicioglu, Y. Gül, and F. Poyraz: Surv. Rev. **55** (2023) 325. https://doi.org/10.1080/00396265.2022.2097998
13 K. Zhang, H. Okazawa, K. Hayashi, T. Hayashi, L. Fiwa, and S. Maskey: Sustainability **14** (2022) 9505. https://doi.org/10.3390/su14159505
14 T. N. Tonkin, and N. G. Midgley: Rem. Sens. **8** (2016) 786. https://doi.org/10.3390/rs8090786
15 E. W. Nota, W. Nijland, and T. de Haas: Int. J. Appl. Earth Obs. Geoinf. **109** (2022) 102772. https://doi.org/10.1016/j.jag.2022.102772
16 Y. Choi, S. Park, and S. Kim: Sensors **22** (2022) 8735. https://doi.org/10.3390/s22228735

About the Authors

Jeongjae Kim received his B.S. and M.S. degrees from Kangwon National University in South Korea in 2021 and 2023, respectively. His research interests include forest environment protection, forest remote sensing, and spatial analysis. (202116435@kangwon.ac.kr)

Ikhyun Kim received his B.S. and M.S. degrees from Kangwon National University in South Korea in 2019 and 2021, respectively. Currently, he is a Ph.D. candidate at Kangwon National University, South Korea. His research interests include forest environment protection, forest soil, and forest engineering. (kih9281@kangwon.ac.kr)

Byoungkoo Choi received his B.S. and M.S. degrees from Kangwon National University in South Korea in 2002 and 2004, respectively, and his Ph.D. degree from Mississippi State University in the USA in 2011. From 2014 to 2015, he was a research scientist at the National Institute of Ecology, South Korea. Since 2015, he has been an associate professor at Kangwon National University. His research interests include eco-hydrology, watershed management, and forestry BMPs. (bkchoi@kangwon.ac.kr)